1-1-1997

The Effects of Sparging on P- and SH- Vertical Seismic Profiles

P. Michaels
Boise State University

W. Barrash
Boise State University

Publication Information

Michaels, P. and Barrash, W. (1997). "The Effects of Sparging on P- and Sh- Vertical Seismic Profiles". In *Symposium on the Application of Geophysics to Engineering and Environmental Problems 1997* (pp. 781-789). The Environmental and Engineering Geophysical Society (EEGS). https://doi.org/10.4133/1.2922456

THE EFFECTS OF SPARGING ON P- AND SH- VERTICAL SEISMIC PROFILES

P. Michaels and W. Barrash
Center of Geophysical Investigation of the Shallow Subsurface
Boise State University
1910 University Drive
Boise, Idaho 83725

ABSTRACT

While the introduction of pressurized air into an unconsolidated, coarse-grained fluvial aquifer might well be expected to affect the P-wave velocity profile below the water table, we have found that S-waves are also sensitive to changes induced by air sparging. In a study spanning over a year of sparging, observations of both P- and S-waves were conducted by Vertical Seismic Profiling (VSP). While the primary objective was to characterize the aquifer, we have found that air sparging has significantly affected both P- and S-wave propagation. Below the water table we have observed as much as a 54% decrease in P-wave velocity, and as much as a 31% increase in S-wave velocity after continued sparging. Above the water table, we observe only small changes in both P- and S-wave velocities. This pattern of velocity change (decreasing P, increasing S) may be due to an increase in the amount of trapped air below the water table.

Published laboratory studies in the small strain regime have shown P-wave velocities to be sensitive to void ratio, fluid content, and confining stress. On the other hand, most similar studies of S-waves have only been conducted on either dry or saturated samples. However, one recent laboratory study suggests that shear modulus and shear velocity may increase significantly at partial water saturations (due to capillary forces). Data from our in-situ survey supports this more recent lab work. We have observed that S-wave propagation may be significantly altered by fluid content when soils are partially saturated with water (where trapped air may exist, producing a 3-phase fluid-frame system). In addition, we have observed changes in the propagating wavelet. This may be an indication that viscous damping is also affected by partial water saturation. We conclude by observing that S-waves may prove to be an attractive alternative for mapping the effects of air sparging.

INTRODUCTION

It is fairly well known that the velocity of a P-wave is significantly affected by the degree of water saturation in a soil or rock. In general, the experience has been that P-wave velocities will decrease with the introduction of even small amounts of air or gas in the pore spaces. This expectation has been confirmed in many studies, both in the laboratory, and in the field (Wyllie et al, 1958, Domenico, 1977, Gregory, 1976). For example, Domenico (1977) observed that the majority of the reduction in P-wave velocity will occur with the introduction of as little as 10% gas into the pores. Such an abrupt effect makes it difficult to use P-wave velocity as an estimator of water saturation.

The usual expectation for S-waves is that water saturation has little effect on the propagation velocity. For soils, void ratio and confining stress are usually considered the major factors governing the speed of an S-wave. In general, a saturated soil should have a slower S-wave velocity than a dry soil, presumably due to the increase in bulk density that results from filling the pores with water (Biot, 1956, Gregory, 1976, Domenico, 1977). However, Gregory (1976) did note that some rocks were anomalous, propagating faster S-waves when saturated with water. We discovered the same phenomena to occur in soils (Michaels and Barrash, 1996). Since our original observation, we have been able to isolate the most probable cause for the effect. This has been made possible by surveying the same soil at two different times. While the frame has remained constant, the fluid saturations have changed as the result of an air sparging operation. Furthermore, it is now clear that laboratory studies on the velocity of S-waves under varying degrees of water saturation appear to be in substantial agreement with our in-situ work. The most probable explanation for the increase in S-wave velocities under partial saturation appears to be related to capillary effects.

Laboratory Observations of S-Velocity at Partial Water Saturations

When comparing laboratory studies to in-situ surveys, it is highly desirable to work in the same frequency range. For our work, this frequency range extends from about 10 to 100 Hz. Thus, we prefer to compare our in-situ survey results with laboratory measurements done by the resonant column method. In this method, a column of soil is excited into vibration (either longitudinally or torsionally). The appropriate velocity is found from the resonant frequency. The apparatus is contained in a pressurized cell so that confinement pressure can be varied. Most published resonant column studies have focused on either dry or saturated soils. In general, studies have shown that S-velocity decreases linearly with increasing void ratio. In addition, under isotropic conditions, the S-velocity increases with the 1/4 power of confining stress (Hardin and Richart, 1963).

Studies of partially saturated soils are far less common. Intuitively, the effects of capillary forces should be relevant. Dry or saturated sand is far less stiff than partially saturated sand (consider the experience of molding sand castles at the beach for example). A study that did explore this effect with a modified resonant column device was conducted by Wu and his colleagues (Wu et al., 1984). Wu found that the shear modulus (and hence, shear velocity) peaked at partial water saturations in the vicinity of 17%. In his Glacier Way Silt sample, the shear modulus increased by a factor of 2 over dry conditions. While Wu correlated the magnitude of the anomalous behavior with effective grain size (D_{10}), it is clear that the pore size is the relevant factor. Thus, Wu notes that the effects could be much larger for soils with plate-shaped particles (presumably since smaller pore sizes would likely result, increasing the influence of capillary forces).

Although Wu chose to display his results in terms of shear modulus, it is not difficult to recast his graphs in terms of shear velocity. For the Glacier Way Silt, Wu proposed a formula of the following form,

$$\frac{G_m}{G_d} = [1+H(S)] \quad . \tag{1}$$

Here, G_m is the moist shear modulus, G_d is the dry shear modulus, and H is an asymmetrical bell shaped function of water saturation, S. This empirically derived function can be recast to give the ratio of moist to dry S-wave velocities. This is done by employing the well known elastic formula for S-wave velocity,

$$V=\sqrt{\frac{G}{\rho}} \quad . \tag{2}$$

Here, V is S-wave velocity and ρ is the bulk density at some degree of water saturation. The bulk density may be re-written in terms of void ratio, e, specific gravity of the grains, Gs, density of water, ρ_w, and water saturation as follows:

$$\rho_m=\frac{(G_s+Se)\,\rho_w}{(1+e)} \quad . \tag{3}$$

Substitution of (2) and (3) into (1) produces the S-wave velocity ratio in terms of the shear modulus ratio,

$$\frac{V_m}{V_d} = \sqrt{\frac{G_m}{G_d}\cdot\left[\frac{G_s}{(G_s+Se)}\right]} \tag{4}$$

Figure 1 shows the application of this transform to Wu's proposed function for the Glacier Way Silt at two different confining pressures (after adjusting his published formula for what appears to be a minor typographical error, see appendix A). As can be seen from the figure, Wu's function predicts slower shear velocities at 100% saturation (compared to dry). This is in agreement with most of the literature. However, at about 17% saturation, he found the Glacier Way Silt exhibited anomalously high shear velocity (due to capillary forces). Also note, the effect is largest at low confining pressures.

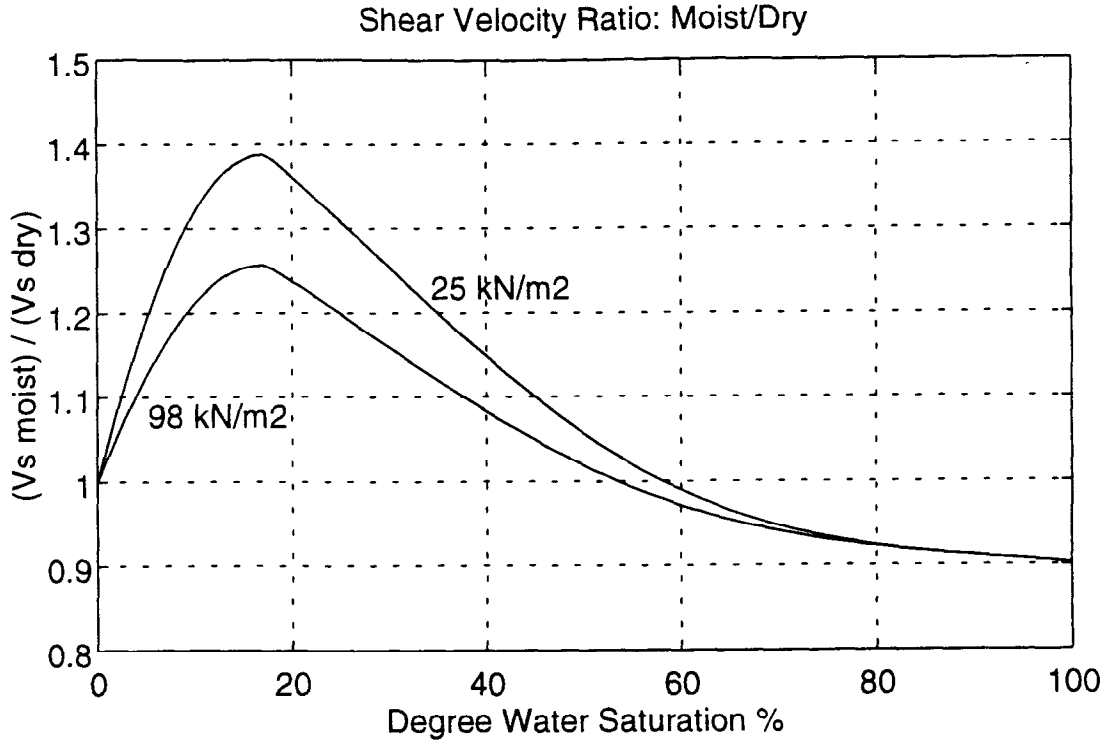

Figure 1. Ratio of moist to dry S-wave velocity expressed by Wu's proposed empirical formula for the Glacier Way Silt (after Wu, 1984). While the magnitude and location of the peak will vary from one soil to the next, the bell shaped nature of the curve seems to be characteristic of capillary effects.

An interesting potential paradox is revealed by Wu's data. The peaked nature of the response measured by Wu illustrates that S-wave velocity will either increase or decrease with increasing water saturation. It depends on what side of the peak one is departing from. For those making in-situ measurements, knowing what side of the peak one is on may be fundamental to using S-waves as a measure of water saturation. Since the location and magnitude of the peak will vary with each soil, we feel that resonant column measurements would be desirable at an early stage of a project in which S-waves might be used to monitor water saturations.

DATA ACQUISITION

As mentioned above, our study was conducted in cooperation with an ongoing water treatment project. We were permitted access to the site during times when the sparging was turned off. Figure 2 shows the timing of our two surveys relative to the sparging work. Note that our first VSP was conducted 4.5 months after the initial pilot program. This was done in the hope of establishing a background condition (after water mounding and dissolved oxygen levels had recovered to near original values). The second VSP was conducted after a year of nearly continuous sparging. A three week off period became available for the VSP. In this second case, far less time had passed from the termination of previous sparging. Thus, the opportunity for trapped air to exist in the soil below the water table is significantly greater for the case of the second VSP. Unfortunately, we have no direct measure of how much trapped air (if any) existed during either survey.

The data for both VSPs were acquired with a Bison 9048 digital seismograph. A sample interval of .0002 seconds was used, filters were set at 4 to 1000 Hz, and 0.5 seconds of data were recorded. The source for the SH-wave experiment was a 1 meter length of railroad tie struck on opposite ends with sledge hammers pivoted by angle iron supports. The P-wave source was a vertical hammer, also pivoted so as to strike a wooden plate in a consistent manner. The source offset was about 1 meter for both surveys.

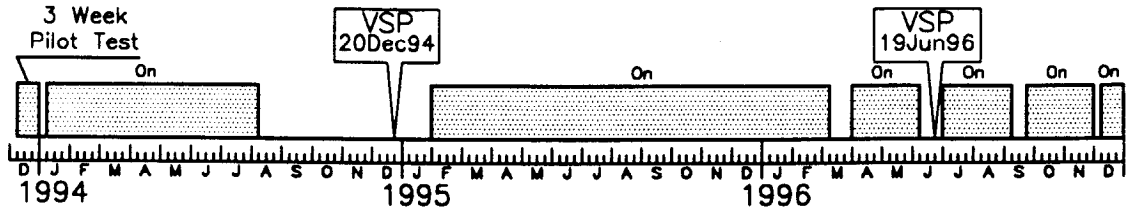

Figure 2. Timing of the VSP acquisition was dependent on the available access to the site between sparging episodes. Over 4.5 months elapsed between sparging and the first VSP. About 2.5 weeks of post sparging time preceded the second VSP. The duration of off time and cumulative sparging lead us to speculate that more trapped air is likely to be present in the second VSP than in the first.

In both surveys, a three component borehole phone, clamped by a metal bow spring was used in the hole (2.5 inch PVC cased). Stations were acquired at 0.5 meter intervals in the first VSP, and 0.25 meter intervals in the second VSP. The second VSP data set have been decimated to the same 0.5 meter interval stations to aid in comparing the two surveys. In addition, a three component reference phone was employed to monitor the consistency of the source efforts. The S-wave data which follow in this paper were taken from the downhole horizontal components. They are the result of the usual subtraction process of opposite polarity source efforts, and a coordinate rotation based on hodogram analysis of the particle motion. The result is the best estimate of the particle motion parallel to the source orientation. The P-wave data were taken from the vertical component of the down hole phone. Triggering of the instrument was by contact closure.

OBSERVED FIRST ARRIVAL TIME DATA

The first step was to pick the first motions of the earliest arrivals. Figure 3 shows these raw picks without any corrections or adjustments. The water table (as measured by the water level in the borehole) was picked at slightly above 815 meters elevation. The ground surface is at +820 meters elevation. Thus, the vadose zone is about 5 meters thick.

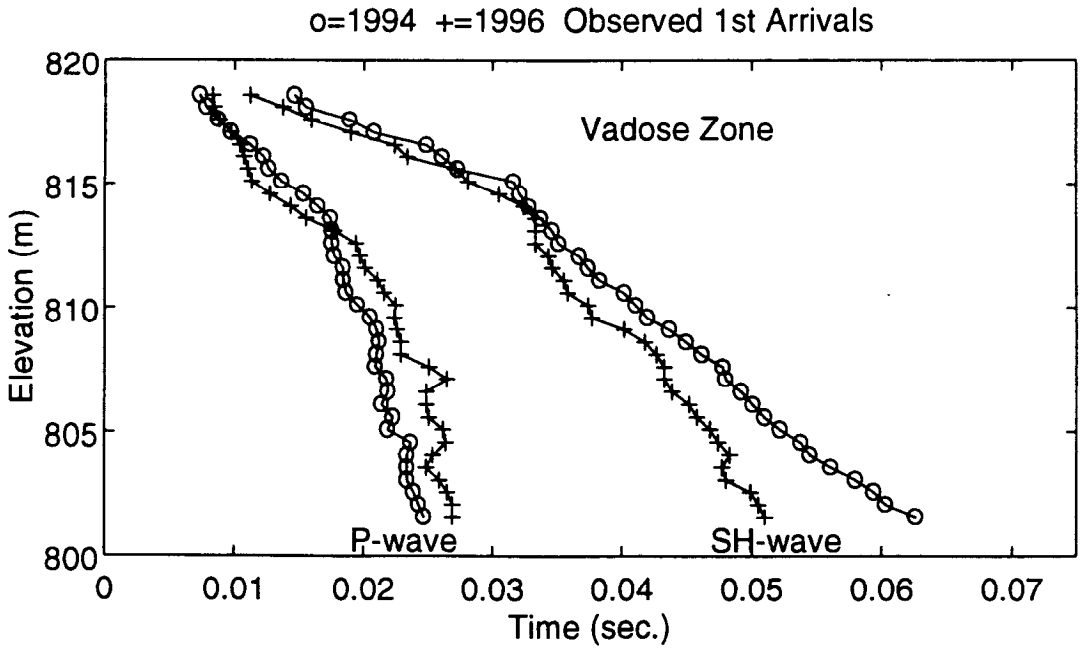

Figure 3. Plots of the first arrival picks. Both S- and P-wave picks are shown. The 1994 VSP data are indicated by circles, and the 1996 data by "+" symbols. Note that after continued sparging, the S-wave arrival times have decreased, and the P-wave times have increased. The water table is at +815 m.

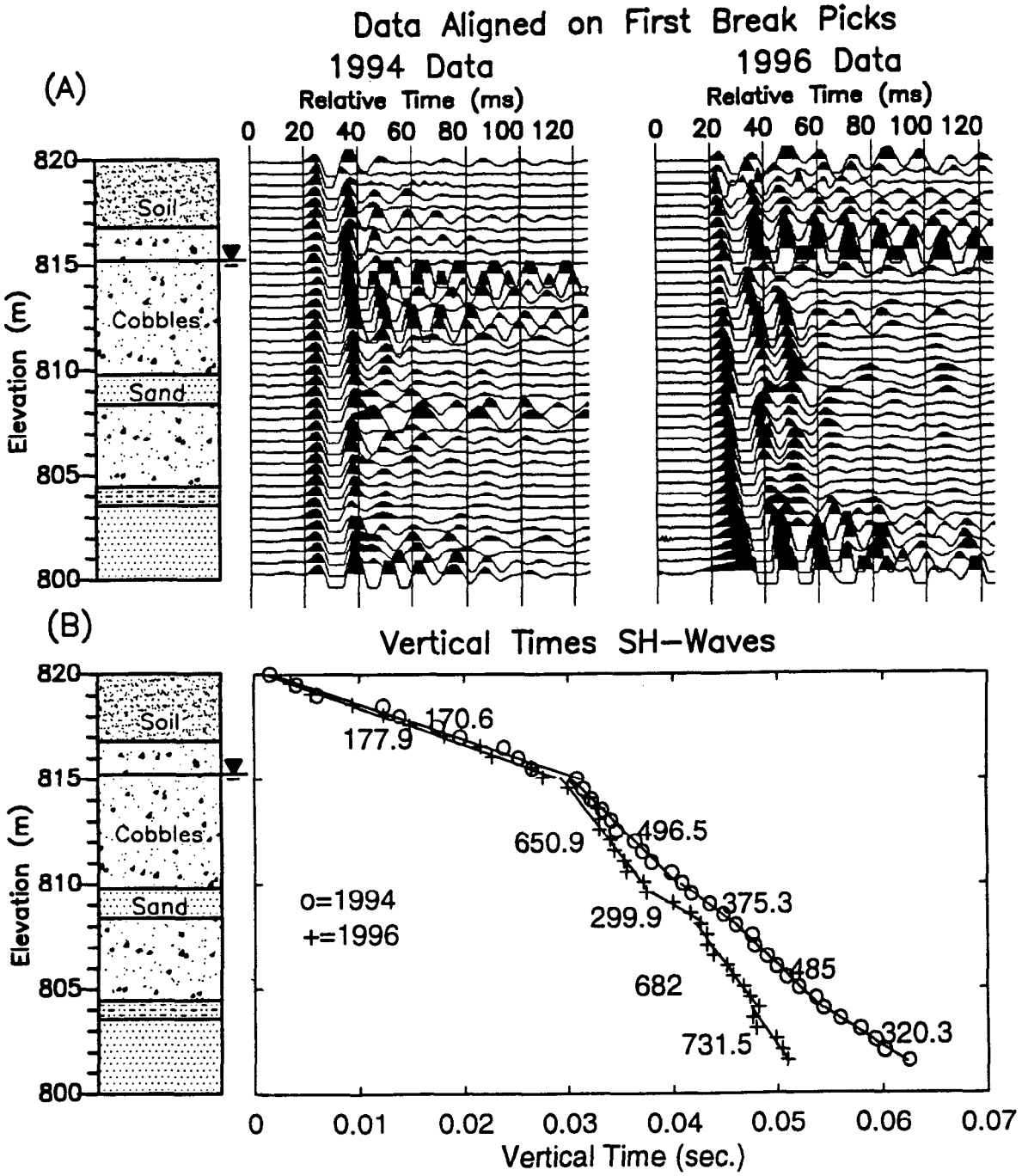

Figure 4. (a) Plot of the S-waves aligned by the first break picks. This permits evaluation of the picking process. (b) Shows the times projected to the vertical. Slopes of line segments fit to the vertical times give the S-wave velocity for selected intervals.

The effect of continued sparging has been to decrease the arrival time of the S-waves. This corresponds to an increase in the wave velocity, possibly due to a change in the water saturation caused by the entrapment of air in the pore spaces. On the other hand, the P-wave arrival times have increased after continued sparging. This behavior would also be consistent with the introduction of trapped air in the pores. To better isolate where velocities have changed, the arrival times were projected to the vertical (cosine projection taking into account the horizontal source offset).

Figure 4a shows the S-wave data shifted into alignment using the first break picks. This provides a

sense of quality control, since a poor pick will result in a waveform shifted from its neighbors. The alignment time is at 20 msec to permit a view of the data before the pick. Figure 4b shows the vertical times computed from the raw picks of the S-wave data. Velocities are determined by fitting straight line segments to linear trends in the vertical times. The slope of the line gives the velocity for the interval being fit by the linear trend. In the vadose zone, there is almost no difference in the interval velocity (shown as 170 or 177 m/s on the plot). The 95% confidence interval is estimated to be +/- 12m/s for these measurements (based on the sum of squared differences between the linear trend and the data). The first major change in velocity occurs just below the water table, in the upper cobble unit. The S-wave velocity increases from 496 to 650 m/s (a 31% increase). The 95% confidence intervals are estimated to be +/- 36m/s and +/-120 m/s for the 1994 and 1996 data respectfully. We also observe changes in the propagating wavelet, suggestive of dispersion and a change in the material damping, assuming a Kelvin model (Michaels, in review). We intend to explore waveform changes in future work.

The upper cobble unit is the most likely zone to have entrapped air. The sparging introduces air at the bottom of a near by injection well. Measurements of dissolved oxygen (Anderson, 1995) indicate an approximately conical region of influence as shown in Figure 5. The cone expands upward toward the water table. The VSP well, situated approximately 15 meters from the injection well, intersects the cone of influence in the upper cobble unit. Assuming that the highest dissolved oxygen region is also the most likely to have entrapped air, we speculate that the upper cobble unit may be producing anomalous S-wave velocities due to a decrease in water saturation (similar to the results shown by Wu (1984) in his study).

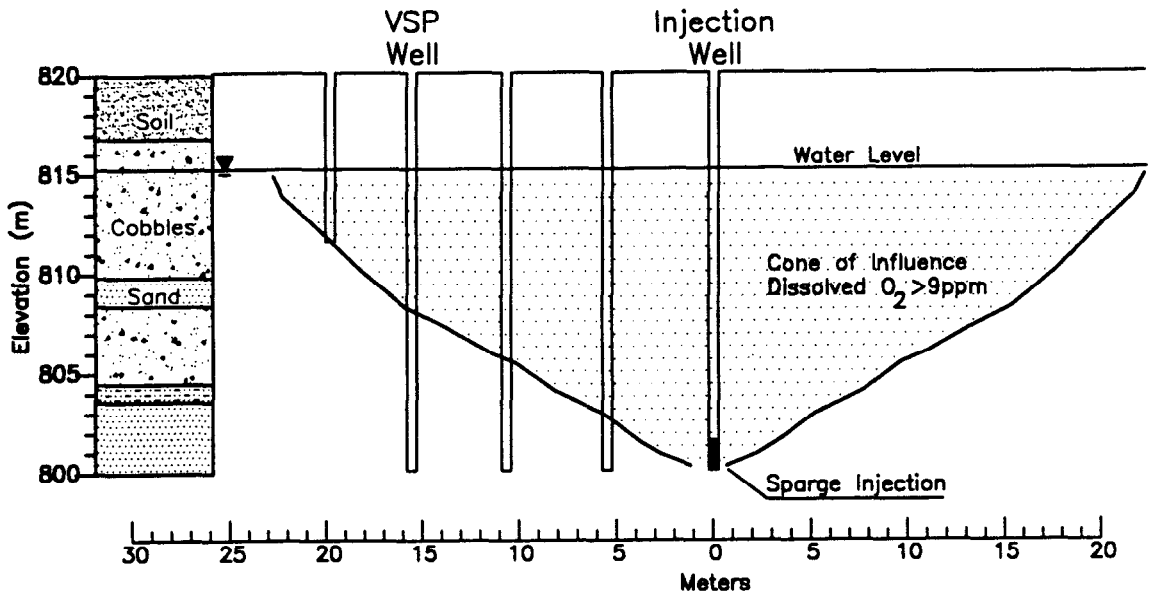

Figure 5. The cone of influence is determined by dissolved oxygen measurements immediately following a period of sparging. The VSP well, located about 15 meters from the injection well, intersects the cone near the water table (after Anderson, 1995).

Figure 6a shows the P-wave data in a display comparable to that of the S-wave data (see Figure 4). Again, the waveforms have been aligned using the first break picks. Much of the later arriving energy is due to S-waves that are unavoidably generated by a vertical hammer source. Also present are reflections (coherent dip up to the right). Figure 6b displays the vertical time data. Again, it appears that the first major change occurs just below the water table where the sparging cone of influence intersects the VSP well. In this case, however, it is the earlier, 1994 data, which exhibit the fastest velocity in the upper cobble unit. After continued sparging, the P-wave velocities decreased from 1696 to 778 m/s (a 54% decrease).

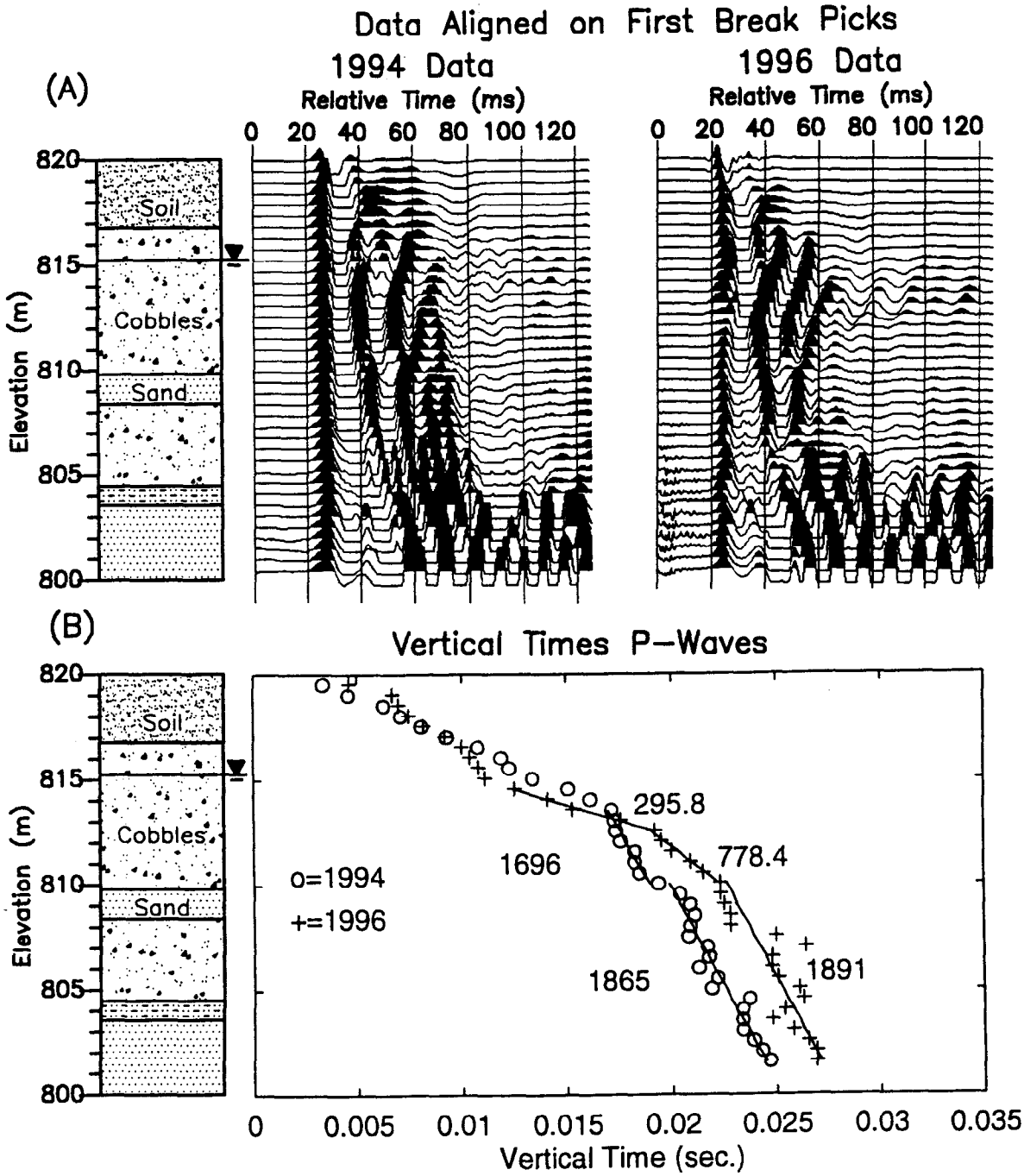

Figure 6. (a) Plot of the P-wave arrivals aligned by the first break picks. This permits evaluation of the picking process. (b) Shows the times projected to the vertical. Slopes of line segments fit to the vertical times give the P-wave velocity for selected intervals.

The 95% confidence intervals for the P-wave velocities in the upper cobble unit are +/- 100 m/s and +/- 400 m/s for the 1994 and 1996 data respectively. Below the upper cobble unit, it appears that there is little difference between the 1994 and 1996 surveys. The velocities obtained in the upper cobble unit are highly suggestive of trapped air, particularly in the context of the S-wave results and the dissolved oxygen measurements. Again, as was the case with the S-waves, there appears to be far less difference in P-wave velocities above the water table than below it.

CONCLUSIONS

By monitoring a site at different times during an air sparging operation, we have observed changes in both P- and S-wave velocities that have likely resulted from changes in the fluid saturations. While the soil frame has remained constant, documented dissolved oxygen measurements suggest that the sparging influence has extended into the well used for VSP acquisition. The decrease in P-wave velocity (54%) and the simultaneous increase in S-wave velocity (31%) in the upper cobble unit are highly suggestive of trapped air in the pores. Furthermore, resonant column laboratory studies have demonstrated that the S-wave behavior observed in our in-situ measurements would be consistent with a reduced degree of water saturation. In that case, the causative mechanism for the S-wave velocity increase would appear to be capillary forces.

In addition to the above observations, we have noticed changes in the waveform of the direct S-wave as it propagates (see Figure 4a). This may be an indication of increased viscous damping. In the future, we hope to explore these dispersion effects in greater detail.

While a sparging operation, by its very nature, is capable of altering the degree of water saturation below the water table, it is possible that these effects may also be observed in natural settings. That is, since most water tables are dynamic (move up and down), the possibility of entrapped air near the water table is significant. In such cases, we would expect an increase in S-wave velocity at the top of the water table.

We conclude by observing that S-waves may be of value in mapping degrees of partial water saturation. Such maps would be useful in monitoring the influence and effects of sparging operations. However, since the effect seems to diminish with increasing confining stress (Wu, 1984), we would expect that the value would be limited to shallow systems, perhaps in the first 20 meters of soil. In any case, resonant column determinations should be made to evaluate this potential use for any particular setting, since the effects can vary significantly with soil type (Wu, 1984).

ACKNOWLEDGEMENTS

The borehole data were acquired with support from the Idaho State Board of Education Specific Research Grant A-037 and by grant DAAH04-94-G-0271 from the U.S. Army Research Office. Views and conclusions contained herein are those of the authors and should not be interpreted as necessarily representing the official policies or endorsements, either expressed or implied, of the Army Research Office or the U.S. Government. We appreciate access to the field site and operational data which have been provided by S-Sixteen Inc. and Anderson Associates Inc. CGISS contribution number 0070.

REFERENCES AND ADDITIONAL READINGS

Anderson, J., 1995, Capitol Station project quarterly report, January-March, Anderson Associates, Boise, Idaho, 125p.

Biot, M. A., 1956, Theory of propagation of elastic waves in a fluid-saturated porous solid. I Low-frequency range. Journal of Acoust. Soc. of America, vol. 28, no. 2, p. 168-178.

Biot, M. A., 1962, Generalized theory of acoustic propagation in porous dissipative media: Journal of Acoust. Soc. of America, vol. 34, no. 9, p. 1254-1264.

Domenico, N., 1977, Elastic properties of unconsolidated porous sand reservoirs: Geophysics, vol. 42, no. 7, p. 1339-1368.

Gregory, A.R., 1976, Fluid saturation effects on dynamic elastic properties of sedimentary rocks: Geophysics, vol. 41, no. 5, p. 895-921.

Hardin, G.O., and Richart, F.E., Jr., 1963, Elastic wave velocities in granular soils, J. Soil Mech. Found. Div., ASCE, Vol. 89, No. SM1, p. 33-65.

Michaels, P., (in review), In-situ measurement of soil stiffness and damping, submitted to the Journal of Geotechnical Engineering, ASCE

Michaels, P. and Barrash, W., 1996, The anomalous behavior of SH-waves across the water table, Proceedings of SAGEEP96, EEGS, Keystone Colorado, p. 137-145.

Wyllie, M.R.J., Gregory, A.R., and Gardner, G.H.F., 1958, Experimental investigation of factors affecting elastic wave velocities in porous media, Geophysics, Vol. 23, No. 3, p. 459-493.

Wu, S., Gray, D.H., and Richart, F.E., Jr., 1984, Capillary effects on dynamic modulus of sands and silts, J. Geotech. Eng. Div., ASCE, Vol 110, No. 9, p. 1188-1203.

APPENDIX A

In reproducing Wu's figure for the Glacier Way Silt, we found it necessary to make a slight change to his published empirical formula for the function H(S) (see equation (1)). H(S) is composed of two parts. One part is for saturations less than the peak. The other is for saturations greater than the peak. The formula for H(S) given by Wu (1984) is:

$$H(S) = (a-1)\sin\left(\frac{\pi S}{2b}\right) \quad , \; S \le b$$

$$H(S) = (a-1)\,H1(S)\,H2(S) \quad , \; S > b$$

where "a" is the maximum amplitude of H(S) and "b" is the water saturation (%) at which the peak occurs. There appears to be a typographical error in the published H1(S) function. Our modified version of Wu's H1(S) is

$$H1(S) = \frac{1}{2}\left(1 - \frac{(S-b)}{(100-b)}\right)^2 \quad .$$

The other part of the formula, H2(S) appears to be correct. For completeness, it is repeated here as

$$H2(S) = \sin\left(\frac{\pi}{(100-b)}\left[S + 50 - \frac{3b}{2}\right]\right) + 1 \quad .$$